

Isotropic Background and Anisotropies of Gravitational Waves Induced by Cosmological Soliton Isocurvature Perturbations

Di Luo,^{a,b} Yan-Heng Yu,^{a,c,*} Jun-Peng Li,^{a,c,*} Sai Wang^{a,*}

^aTheoretical Physics Division, Institute of High Energy Physics, Chinese Academy of Sciences, 19B Yuquan Road, Shijingshan District, Beijing 100049, China

^bSchool of Physical Sciences, University of Science and Technology of China, 96 Jinzhai Road, Baohe District, Hefei 230026, China

^cSchool of Physics, University of Chinese Academy of Sciences, 19A Yuquan Road, Shijingshan District, Beijing 100049, China

E-mail: luo1844725234@mail.ustc.edu.cn, yhyu@ihep.ac.cn, lijunpeng@ihep.ac.cn, wangsai@ihep.ac.cn

Abstract. Cosmological solitons are widely predicted by scenarios of the early Universe. In this work, we investigate the isotropic background and anisotropies of gravitational waves (GWs) induced by soliton isocurvature perturbations, especially considering the effects of non-Gaussianity in these perturbations. Regardless of non-Gaussianity, the energy-density fraction spectrum of isocurvature-induced GWs approximately has a universal shape within the perturbative regime, thus serving as a distinctive signal of solitons. We derive the angular power spectrum of isocurvature-induced GWs to characterize their anisotropies. Non-Gaussianity plays a key role in generating anisotropies through the couplings between large- and small-scale isocurvature perturbations, making the angular power spectrum to be a powerful probe of non-Gaussianity. Moreover, the isocurvature-induced GWs have nearly no cross-correlations with the cosmic microwave background, providing a new observable to distinguish them from other GW sources, e.g., GWs induced by cosmological curvature perturbations enhanced at small scales. Therefore, detection of both the isotropic background and anisotropies of isocurvature-induced GWs could reveal important implications for the solitons as well as the early Universe.

*Corresponding author.

Contents

1	Introduction	1
2	Cosmological isocurvature perturbations from solitons	2
3	Isotropic background of isocurvature-induced GWs	4
3.1	Energy-density fraction spectrum	5
3.2	Numerical results	7
4	Anisotropies of isocurvature-induced GWs	9
4.1	Reduced angular power spectrum	9
4.2	Numerical results	11
5	Conclusions and discussion	13
A	Formulas for the energy-density fraction spectrum	15

1 Introduction

The long-lived localized massive objects, known as “solitons”, are prevalent in a variety of scenarios of the early Universe and have garnered significant interest. These solitons, including topological defects, oscillons, Q-balls, etc., can naturally arise in cosmological models containing new physics (e.g., see review [1] and references therein), or are introduced to address fundamental issues like dark matter (e.g., see Ref. [2]). Exploring the properties of solitons holds essential implications for comprehending the early Universe.

The cosmological isocurvature perturbations contain rich information about solitons in the early Universe. At the formation time, solitons generally have little impact on the total energy density of the Universe, primarily introducing relative inhomogeneities among different components, thereby acting as isocurvature perturbations. These perturbations are orthogonal to the cosmological curvature perturbations, with the latter arising from the perturbations to the radiation that dominates the evolution of the early Universe. At large scales, the spectral amplitude of isocurvature perturbations is less than $\sim 1\%$ of that of curvature ones, as constrained by observations of the cosmic microwave background (CMB) [3]. However, the universal characteristics of the solitons can lead to enhanced isocurvature perturbations at much smaller scales associated with their typical non-linear scales [4], providing a valuable avenue for studying solitons.

Reflecting deviations from the Gaussian statistics, the non-Gaussianity is one of the most important natures of the soliton isocurvature perturbations. Just as the non-Gaussianity in curvature perturbations provides insights into inflationary dynamics [5–16], the non-Gaussianity in soliton isocurvature perturbations offers a distinctive window into the underlying dynamics of the fields related to these solitons. Detecting such non-Gaussianity at large scales would confront challenges since the isocurvature perturbations are constrained to be small. On the other hand, detecting it at small scales, though lacking tight constraints, necessitates the development of new detection approaches.

Gravitational waves (GWs) induced by isocurvature perturbations provide a new probe of the solitons. In contrast to GWs induced by curvature perturbations, which are known as “scalar-induced gravitational waves (SIGWs)” [17–23], GWs can not be induced directly by isocurvature perturbations, since they do not affect the shape of space by definition. However, if the energy-density fractions of the matter ingredients in the Universe undergo changes, the initial isocurvature perturbations may partially evolve into curvature perturbations, leading to the inevitable generation of GWs due to nonlinear effects of gravity [24]. These so-called “isocurvature-induced GWs” can be generally produced from cosmological solitons [4]. Since the solitons behave as the non-relativistic matter, their energy density decays slower than that of radiation as the Universe expands. With the energy-density fraction of solitons growing, the initial soliton isocurvature perturbations at small scales transform into curvature ones, and act as the sources of GWs. Other relevant works of the isocurvature-induced GWs can also be found in the literature [25–36].

Identifying the non-Gaussianity in soliton isocurvature perturbations via the isocurvature-induced GWs remains one of the important research objectives. This study will delve into both the isotropic background and anisotropies of isocurvature-induced GWs, with a specific focus on the effects of non-Gaussianity. As for the isotropic background, Ref. [4] shows that for a wide class of solitons, the corresponding isocurvature-induced GWs share the same shape of energy-density fraction spectrum, known as “universal GWs”. We will reveal that this energy-density fraction spectrum is insensitive to non-Gaussianity in isocurvature perturbations within the perturbative regime, indicating that this “universal GWs” could still serve as a distinctive signal for detecting these solitons, irrespective of whether the isocurvature perturbations are Gaussian or not. This differs from the case of SIGWs, whose energy-density fraction spectrum can experience significant modifications due to the non-Gaussianity in primordial curvature perturbations [37–61]. To extract the information of non-Gaussianity, we will further study the anisotropies of isocurvature-induced GWs and derive the (reduced) angular power spectrum. Analogous to the analysis of anisotropies in SIGWs [42–46, 62–67], the non-Gaussianity in isocurvature perturbations will be shown to play a critical role in generating the anisotropies of isocurvature-induced GWs, and notably affect the angular power spectrum. Therefore, these anisotropies could be an effective probe of the non-Gaussianity in isocurvature perturbations, breaking its degeneracy with other model parameters and shedding light on the dynamics associated with solitons. Furthermore, we will demonstrate that cross-correlations between GWs and the CMB, could offer features distinct from other GW sources, e.g., SIGWs [64, 68, 69], serving as novel signals to identify solitons.

The rest of this paper is structured as follows. In Section 2, we review the cosmological isocurvature perturbations due to solitons. In Section 3, we investigate the energy-density fraction spectrum of isocurvature-induced GWs, considering the effects of non-Gaussianity in soliton isocurvature perturbations. In Section 4, we analyze the angular power spectrum of isocurvature-induced GWs, and focus on its implications for detecting the non-Gaussianity in soliton isocurvature perturbations. Moreover, we compare our results to those of SIGWs. In Section 5, we reveal the conclusions and discussion. In Appendix A, we summarize the formulas for the energy-density fraction spectrum necessary for Section 3.

2 Cosmological isocurvature perturbations from solitons

Similar to Ref. [4], we consider an early Universe comprising two fluids, namely, radiation originating from the inflaton decay, and solitons formed by a spectator field which is only

weakly coupled to the inflaton. When solitons form, the energy density of radiation greatly exceeds that of solitons, resulting in a radiation-dominated (RD) era. While fluctuations in radiation contribute to cosmological curvature perturbations, the Poisson distribution of solitons gives rise to enhanced cosmological isocurvature perturbations at small scales. As the energy-density fraction of solitons increases with the Universe’s expansion, these isocurvature perturbations gradually evolve into curvature ones, acting as sources of GWs in the RD era, termed “isocurvature-induced GWs”. Further, if solitons are long-lived enough, they could initiate a soliton-dominated era at some time. This soliton-dominated era would transit into the standard RD era when solitons eventually decay, which may lead to significant production of GWs, depending on whether this transition is sudden or not [70–72]. However, to avoid getting stuck in a discussion about the details of the soliton-dominated era, which is not the primary focus of our present paper, we assume that the solitons decay at around the radiation-soliton equality, resulting in the absence of soliton domination.

Let us focus on the cosmological perturbations first. We consider a perturbed Friedmann-Robertson-Walkers (FRW) metric in the conformal Newtonian gauge, i.e.,

$$ds^2 = a^2(\eta) \left\{ -(1 + 2\Phi) d\eta^2 + \left[(1 - 2\Phi)\delta_{ij} + \frac{1}{2}h_{ij} \right] dx^i dx^j \right\}. \quad (2.1)$$

Here, $a(\eta)$ is a scale factor of the Universe at the conformal time η , and is given by $a(\eta)/a_{\text{eeq}} = 2\eta/\eta_* + (\eta/\eta_*)^2$ in the radiation-soliton Universe, where $\eta_* = (\sqrt{2} + 1)\eta_{\text{eeq}}$, and the subscript “eeq” denotes the radiation-soliton equality. The Φ denotes the first-order cosmological scalar perturbations with the anisotropic stress being neglected, and is proportional to the linear cosmological curvature perturbations ζ . The h_{ij} stands for the second-order transverse-traceless tensor perturbations, which will be studied in the subsequent sections. Moreover, the cosmological isocurvature perturbations \mathcal{S} do not affect the spacetime metric, and is defined in a gauge-invariant form as [73, 74]

$$\mathcal{S} = \frac{\delta\rho_m}{\rho_m} - \frac{3}{4} \frac{\delta\rho_r}{\rho_r}, \quad (2.2)$$

where ρ_m (or ρ_r) is the energy density of solitons (or radiation), and $\delta\rho_m$ (or $\delta\rho_r$) is the fluctuations in ρ_m (or ρ_r). It should be noted that \mathcal{S} can be roughly determined by the density contrast of solitons during the RD era, namely $\mathcal{S} \simeq \delta\rho_m/\rho_m$, considering $\rho_m \ll \rho_r$ and the isocurvature condition $\delta\rho_m + \delta\rho_r = 0$ in Eq. (2.2).

We investigate ζ and \mathcal{S} at the initial conformal time η_i when solitons form. Different from Ref. [4], we consider the non-Gaussianity in \mathcal{S} , which can result from some dynamic mechanism of the field related to soliton formation, whereas we neglect the non-Gaussianity in ζ . We further assume that the non-Gaussian \mathcal{S} is parameterized in the Fourier space as

$$\mathcal{S}(\eta_i, \mathbf{k}) = \mathcal{S}_g(\eta_i, \mathbf{k}) + F_{\text{NL,iso}} \int \frac{d^3\mathbf{q}}{(2\pi)^{3/2}} \mathcal{S}_g(\eta_i, \mathbf{q}) \mathcal{S}_g(\eta_i, \mathbf{k} - \mathbf{q}), \quad (2.3)$$

where \mathbf{k} and \mathbf{q} are the Fourier modes of perturbations, \mathcal{S}_g stands for the Gaussian component of \mathcal{S} , and $F_{\text{NL,iso}}$ is the non-linearity parameter of \mathcal{S} . In this work, we focus solely on the non-Gaussianity up to the order of $F_{\text{NL,iso}}$, but the effects of higher-order non-Gaussianity can be straightforwardly extended to, following the framework established in Refs. [39–41, 43, 44]. In order to describe the statistics of Gaussian variables ζ and \mathcal{S}_g , we introduce their dimensionless power spectra as follows

$$\langle \zeta(\eta_i, \mathbf{k}_1) \mathcal{S}_g(\eta_i, \mathbf{k}_2) \rangle = 0, \quad (2.4)$$

$$\langle \zeta(\eta_i, \mathbf{k}_1) \zeta(\eta_i, \mathbf{k}_2) \rangle = \delta^{(3)}(\mathbf{k}_1 + \mathbf{k}_2) \frac{2\pi^2}{k_1^3} \Delta_\zeta^2(k_1), \quad (2.5)$$

$$\langle \mathcal{S}_g(\eta_i, \mathbf{k}_1) \mathcal{S}_g(\eta_i, \mathbf{k}_2) \rangle = \delta^{(3)}(\mathbf{k}_1 + \mathbf{k}_2) \frac{2\pi^2}{k_1^3} \Delta_{\mathcal{S}_g}^2(k_1), \quad (2.6)$$

where we have $k = |\mathbf{k}|$, and $\langle \dots \rangle$ represents the ensemble average. In this work, the correlator in Eq. (2.4) is expected to vanish, since ζ and \mathcal{S}_g are assumed to have uncorrelated origins. We adopt a scale-invariant Δ_ζ^2 in Eq. (2.5) with the spectral amplitude $\mathcal{A}_{\text{ad}} \simeq 2.1 \times 10^{-9}$ that is revealed by the Planck 2018 results [75]. In contrast, $\Delta_{\mathcal{S}_g}^2$ in Eq. (2.6) is modeled as

$$\Delta_{\mathcal{S}_g}^2(k) = \mathcal{A}_{L,\text{iso}} + \mathcal{A}_{S,\text{iso}} \left(\frac{k}{k_{\text{uv}}} \right)^3 \Theta(k_{\text{uv}} - k), \quad (2.7)$$

where the subscript “ L ” (or “ S ”) represents large (or small) scales, and a cutoff scale k_{uv} is introduced to maintain the validity of our “soliton fluid” description. At large scales, \mathcal{S}_{gL} has a scale-invariant spectral amplitude $\mathcal{A}_{L,\text{iso}}$ with the constraint $\beta = \mathcal{A}_{L,\text{iso}}/\mathcal{A}_{\text{ad}} \lesssim 10^{-2}$ based on observations of the CMB temperature anisotropies and polarization [3]. At small scales $k \lesssim k_{\text{uv}}$, \mathcal{S}_{gS} follows a k^3 -spectrum due to the Poisson distribution of solitons, and the spectral amplitude at $k = k_{\text{uv}}$ can be enhanced to $\mathcal{A}_{S,\text{iso}} \sim \mathcal{O}(1)$ [4].

We then focus on how the small-scale isocurvature perturbations evolve into curvature ones at η , which satisfies $\eta_i < \eta \ll \eta_{\text{eeq}}$. Deep in the RD era, the equations of motion of Φ and \mathcal{S} are given by [4, 24]

$$\frac{d^2\Phi}{dx^2} + \frac{4}{x} \frac{d\Phi}{dx} + \frac{1}{3}\Phi + \frac{1}{4\sqrt{2}\kappa x} \left[x \frac{d\Phi}{dx} + (1-x^2)\Phi - 2\mathcal{S} \right] \simeq 0, \quad (2.8)$$

$$\frac{d^2\mathcal{S}}{dx^2} + \frac{1}{x} \frac{d\mathcal{S}}{dx} - \frac{x^2}{6}\Phi - \frac{1}{2\sqrt{2}\kappa} \left(\frac{d\mathcal{S}}{dx} - \frac{x}{2}\mathcal{S} - \frac{x^3}{12}\Phi \right) \simeq 0. \quad (2.9)$$

Here, we introduce the dimensionless parameters $x = k\eta \gg 1$ and $\kappa = k/k_{\text{eeq}}$ with $x/\kappa \ll 1$, where k_{eeq} is related to the mode reentering the horizon at η_{eeq} . To solve the above equations, we approximately set the initial conditions as $\Phi = 0$ and $\mathcal{S} = \mathcal{S}(\eta_i, \mathbf{k})$ because of $\mathcal{A}_{\text{ad}} \ll \mathcal{A}_{S,\text{iso}}$. The analytical solutions of Eqs. (2.8) and (2.9) up to order $(x/\kappa)^2$ are given by [4, 24]

$$\Phi(\eta, \mathbf{k}) \simeq \frac{3\mathcal{S}(\eta_i, \mathbf{k})}{2\sqrt{2}\kappa} \frac{1}{x^3} \left[6 + x^2 - 2\sqrt{3}x \sin\left(\frac{x}{\sqrt{3}}\right) - 6 \cos\left(\frac{x}{\sqrt{3}}\right) \right], \quad (2.10)$$

$$\mathcal{S}(\eta, \mathbf{k}) \simeq \mathcal{S}(\eta_i, \mathbf{k}) + \frac{3\mathcal{S}(\eta_i, \mathbf{k})}{2\sqrt{2}\kappa} \left[x + \sqrt{3} \sin\left(\frac{x}{\sqrt{3}}\right) - 2\sqrt{3} \text{Si}\left(\frac{x}{\sqrt{3}}\right) \right], \quad (2.11)$$

where $\text{Si}(x)$ is the sine-integral function. Though these solutions are derived in the condition $\eta_i = 0$, they are still applicable for the case $\eta_i > 0$ [4]. As demonstrated in Eq. (2.10), the $\mathcal{S}(\eta_i, \mathbf{k})$ could evolve into the scalar perturbations Φ or correspondingly the curvature perturbations ζ , which are the sources of GWs studied below.

3 Isotropic background of isocurvature-induced GWs

As the soliton isocurvature perturbations evolve into curvature perturbations during the RD era, the subsequent evolution of the latter inside the horizon inevitably induces GWs, known

as "isocurvature-induced GWs", i.e., the h_{ij} in Eq. (2.1). The energy density of these GWs is defined by

$$\rho_{\text{gw}}(\eta, \mathbf{x}) = \frac{M_{\text{pl}}^2}{16 a^2(\eta)} \overline{\partial_l h_{ij}(\eta, \mathbf{x}) \partial_l h_{ij}(\eta, \mathbf{x})} , \quad (3.1)$$

where \mathbf{x} is a spatial position, the long overbar represents oscillation average, and M_{pl} is the reduced Planck mass. We further decompose ρ_{gw} as

$$\rho_{\text{gw}}(\eta, \mathbf{x}) = \bar{\rho}_{\text{gw}}(\eta) + \delta\rho_{\text{gw}}(\eta, \mathbf{x}) , \quad (3.2)$$

where $\bar{\rho}_{\text{gw}}$ refers to the isotropic background, i.e., the spatial average of $\rho_{\text{gw}}(\eta, \mathbf{x})$, and $\delta\rho_{\text{gw}}$ denotes the fluctuations on top of this background. In order to characterize $\bar{\rho}_{\text{gw}}$ and $\delta\rho_{\text{gw}}$, we define the energy-density fraction spectrum $\bar{\Omega}_{\text{gw}}(\eta, \mathbf{x})$ and the density contrast $\delta_{\text{gw}}(\eta, \mathbf{x}, \mathbf{k})$, respectively, i.e., [76, 77]

$$\bar{\Omega}_{\text{gw}}(\eta, k) = \frac{1}{\rho_c(\eta)} \frac{d\bar{\rho}_{\text{gw}}(\eta)}{d \ln k} , \quad (3.3a)$$

$$\delta_{\text{gw}}(\eta, \mathbf{x}, \mathbf{k}) = \frac{1}{\rho_c(\eta)} \frac{4\pi}{\bar{\Omega}_{\text{gw}}(\eta, k)} \frac{d\delta\rho_{\text{gw}}(\eta, \mathbf{x})}{d \ln k d^2 \hat{\mathbf{k}}} , \quad (3.3b)$$

where $\rho_c(\eta)$ is the critical energy density of the Universe at η , \mathbf{k} is the wavevector of GWs with $\hat{\mathbf{k}} = \mathbf{k}/k$ being the unit directional vector.

In this section, we focus on $\bar{\Omega}_{\text{gw}}$, which describes the homogeneous and isotropic background of GWs. In the subsequent section, we will study $\delta_{\text{gw}}(\eta, \mathbf{x}, \mathbf{k})$, which results in the inhomogeneities and anisotropies in GWs.

3.1 Energy-density fraction spectrum

The energy-density fraction spectrum of isocurvature-induced GWs can be computed using a semi-analytical approach akin to that employed for SIGWs [17–23]. In Fourier space, h_{ij} is expressed as

$$h_{ij}(\eta, \mathbf{x}) = \sum_{\lambda=+, \times} \int \frac{d^3 \mathbf{k}}{(2\pi)^{3/2}} e^{i\mathbf{k}\cdot\mathbf{x}} \epsilon_{ij, \mathbf{k}}^\lambda h_\lambda(\eta, \mathbf{k}) , \quad (3.4)$$

where $\lambda = +, \times$ are two polarization modes of GWs, and the polarization tensors are defined as $\epsilon_{ij, \mathbf{k}}^+ = [\epsilon_{i, \mathbf{k}} \epsilon_{j, \mathbf{k}} - \bar{\epsilon}_{i, \mathbf{k}} \bar{\epsilon}_{j, \mathbf{k}}]/\sqrt{2}$ and $\epsilon_{ij, \mathbf{k}}^\times = [\epsilon_{i, \mathbf{k}} \epsilon_{j, \mathbf{k}} + \bar{\epsilon}_{i, \mathbf{k}} \bar{\epsilon}_{j, \mathbf{k}}]/\sqrt{2}$ with $\epsilon_{i, \mathbf{k}}$ and $\bar{\epsilon}_{i, \mathbf{k}}$ forming an orthonormal basis perpendicular to \mathbf{k} . The equation of motion of $h_\lambda(\eta, \mathbf{k})$ is given by

$$h_\lambda''(\eta, \mathbf{k}) + 2\mathcal{H}h_\lambda'(\eta, \mathbf{k}) + k^2 h_\lambda(\eta, \mathbf{k}) = 4\mathcal{T}_\lambda(\eta, \mathbf{k}) , \quad (3.5)$$

where a prime stands for a derivative with respect to η . The source term $\mathcal{T}_\lambda(\eta, \mathbf{k})$ is given by

$$\mathcal{T}_\lambda(\eta, \mathbf{k}) = \int \frac{d^3 \mathbf{q}}{(2\pi)^{3/2}} Q_\lambda(\mathbf{k}, \mathbf{q}) f(|\mathbf{k} - \mathbf{q}|, q, \eta) \mathcal{S}(\eta_i, \mathbf{k} - \mathbf{q}) \mathcal{S}(\eta_i, \mathbf{q}) , \quad (3.6)$$

where $Q_\lambda(\mathbf{k}, \mathbf{q}) = \epsilon_{ij, \mathbf{k}}^\lambda(\mathbf{k}) q_i q_j$ denotes a projection factor, and $f(|\mathbf{k} - \mathbf{q}|, q, \eta)$ is given by

$$f(p, q, \eta) = 2T(p, \eta)T(q, \eta) + [T(p, \eta) + \eta T'(p, \eta)] [T(q, \eta) + \eta T'(q, \eta)] , \quad (3.7)$$

where we introduce $p = |\mathbf{k} - \mathbf{q}|$, and the transfer function $T(\eta, k)$ connects $\Phi(\eta, \mathbf{k})$ and the initial isocurvature perturbations $\mathcal{S}(\eta_i, \mathbf{k})$, i.e.,

$$\Phi(\eta, \mathbf{k}) = T(\eta, k) \mathcal{S}(\eta_i, \mathbf{k}) . \quad (3.8)$$

The explicit expression of $T(\eta, k)$ can be straightforwardly read from Eq. (2.10), i.e.,

$$T(\eta, k) \simeq \frac{3}{2\sqrt{2}x^3\kappa} \left[6 + x^2 - 2\sqrt{3}x \sin\left(\frac{x}{\sqrt{3}}\right) - 6 \cos\left(\frac{x}{\sqrt{3}}\right) \right]. \quad (3.9)$$

Following the Green's function method [22, 23], the solution to Eq. (3.5) is formally given by

$$h_\lambda(\eta, \mathbf{k}) = \frac{4}{k^2} \int \frac{d^3\mathbf{q}}{(2\pi)^{3/2}} Q_\lambda(\mathbf{k}, \mathbf{q}) \hat{I}\left(\frac{|\mathbf{k}-\mathbf{q}|}{k}, \frac{q}{k}, \kappa, x\right) \mathcal{S}(\eta_i, \mathbf{k}-\mathbf{q}) \mathcal{S}(\eta_i, \mathbf{q}), \quad (3.10)$$

where the kernel function $\hat{I}(u, v, \kappa, x)$ with $x \gg 1$ is given by¹ [24]

$$\hat{I}(u, v, \kappa, x \gg 1) = \frac{1}{x} I_A(u, v, \kappa) [I_B(u, v) \sin x - \pi I_C(u, v) \cos x], \quad (3.11a)$$

$$I_A(u, v, \kappa) = 9 / (16u^4v^4\kappa^2), \quad (3.11b)$$

$$\begin{aligned} I_B(u, v) = & -3u^2v^2 + (-3 + u^2)(-3 + u^2 + 2v^2) \ln \left| 1 - \frac{u^2}{3} \right| \\ & + (-3 + v^2)(-3 + v^2 + 2u^2) \ln \left| 1 - \frac{v^2}{3} \right| \\ & - \frac{1}{2} (-3 + v^2 + u^2)^2 \ln \left[\left| 1 - \frac{(u+v)^2}{3} \right| \left| 1 - \frac{(u-v)^2}{3} \right| \right], \quad (3.11c) \end{aligned}$$

$$\begin{aligned} I_C(u, v) = & 9 - 6v^2 - 6u^2 + 2u^2v^2 \\ & + (3 - u^2)(-3 + u^2 + 2v^2) \Theta\left(1 - \frac{u}{\sqrt{3}}\right) \\ & + (3 - v^2)(-3 + v^2 + 2u^2) \Theta\left(1 - \frac{v}{\sqrt{3}}\right) \\ & + \frac{1}{2} (-3 + v^2 + u^2)^2 \left[\Theta\left(1 - \frac{u+v}{\sqrt{3}}\right) + \Theta\left(1 + \frac{u-v}{\sqrt{3}}\right) \right]. \quad (3.11d) \end{aligned}$$

Note that the kernel function of isocurvature-induced GWs exhibits a factor of κ^{-2} , which is different from the case for SIGWs [22, 23].

At the conformal time of GW emission, denoted as η_e , the energy-density fraction spectrum of isocurvature-induced GWs, denoted as $\bar{\Omega}_{\text{gw},e}(k) = \bar{\Omega}_{\text{gw}}(\eta_e, k)$ for simplicity, can be obtained from Eq. (3.3a), i.e.,

$$\bar{\Omega}_{\text{gw},e}(k) = \frac{1}{48} \left[\frac{k}{\mathcal{H}(\eta_e)} \right]^2 \sum_{\lambda=+, \times} \overline{\Delta_\lambda^2(\eta_e, k)}, \quad (3.12)$$

where $\mathcal{H}(\eta_e)$ is the conformal Hubble parameter at η_e , and the dimensionless power spectrum of GWs is defined as

$$\langle h_{\lambda_1}(\eta_e, \mathbf{k}_1) h_{\lambda_2}(\eta_e, \mathbf{k}_2) \rangle = \delta_{\lambda_1 \lambda_2} \delta^{(3)}(\mathbf{k}_1 + \mathbf{k}_2) \frac{2\pi^2}{k_1^3} \Delta_{\lambda_1}^2(\eta_e, k_1). \quad (3.13)$$

¹The analytical expressions in Eq. (3.11) are derived under the condition $k_{\text{uv}}\eta_i \rightarrow 0$. For $k_{\text{uv}}\eta_i \gtrsim 1$, the kernel function lacks simple expressions. In this work, we adopt the result in Eq. (3.11) as an approximation. Numerical analysis indicates that the change of the energy-density fraction spectrum within the range of $0 < k_{\text{uv}}\eta_i \lesssim 10$ is less than $\sim 30\%$, which would not affect our main results.

Based on Eqs. (3.10), (3.12), and (3.13), we have $\bar{\Omega}_{\text{gw},e} \sim \langle h^2 \rangle \sim \langle \mathcal{S}^4 \rangle \simeq \langle \mathcal{S}_S^4 \rangle$, where the non-Gaussian \mathcal{S}_S is given by $\mathcal{S}_S \sim \mathcal{S}_{gS} + F_{\text{NL},\text{iso}} \mathcal{S}_{gS}^2$ based on Eq. (2.3), and we can safely neglect the contribution from \mathcal{S}_{gL} because of $\mathcal{A}_{L,\text{iso}} \ll \mathcal{A}_{S,\text{iso}}$. According to the Wick's theorem, the four-point correlator $\langle \mathcal{S}_S^4 \rangle$ can be expanded in terms of the two-point correlator $\langle \mathcal{S}_{gS}^2 \rangle$. To simplify this calculation, we could apply a diagrammatic approach [37–39, 41–44, 53, 63, 78–80], which is well-established in the study of the non-Gaussianity of curvature perturbations in the case of SIGWs. As a result, $\bar{\Omega}_{\text{gw}}$ is expressed as

$$\bar{\Omega}_{\text{gw},e} = \bar{\Omega}_{\text{gw},e}^{(0)} + \bar{\Omega}_{\text{gw},e}^{(1)} + \bar{\Omega}_{\text{gw},e}^{(2)}, \quad (3.14)$$

where $\bar{\Omega}_{\text{gw},e}^{(n)}$ ($n = 0, 1, 2$) denotes the $\mathcal{O}(\mathcal{A}_{S,\text{iso}}^{n+2} F_{\text{NL},\text{iso}}^{2n})$ component of $\bar{\Omega}_{\text{gw},e}$, i.e.,

$$\bar{\Omega}_{\text{gw},e}^{(0)} = \bar{\Omega}_{\text{gw},e}^G, \quad (3.15a)$$

$$\bar{\Omega}_{\text{gw},e}^{(1)} = \bar{\Omega}_{\text{gw},e}^H + \bar{\Omega}_{\text{gw},e}^C + \bar{\Omega}_{\text{gw},e}^Z, \quad (3.15b)$$

$$\bar{\Omega}_{\text{gw},e}^{(2)} = \bar{\Omega}_{\text{gw},e}^R + \bar{\Omega}_{\text{gw},e}^P + \bar{\Omega}_{\text{gw},e}^N. \quad (3.15c)$$

The explicit expressions of $\bar{\Omega}_{\text{gw},e}^X$ ($X = G, H, C, Z, R, P, N$) are listed in Appendix A. We note that their expressions share the same form as those of SIGWs except for the different specific expressions of the kernel functions [37–48, 81].

3.2 Numerical results

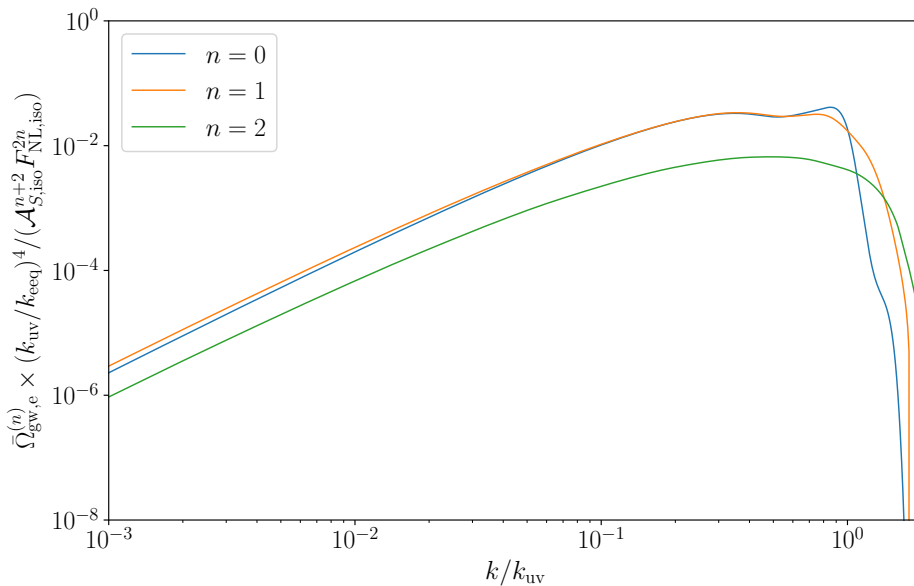


Figure 1. Unscaled components of the energy-density fraction spectrum of isocurvature-induced GWs as a function of the scale k/k_{uv} .

In Fig. 1, we present the unscaled components of the energy-density fraction spectrum of isocurvature-induced GWs, namely $\bar{\Omega}_{\text{gw},e}^{(n)} \times (k_{\text{uv}}/k_{\text{eeq}})^4 \times (\mathcal{A}_{S,\text{iso}}^{n+2} F_{\text{NL},\text{iso}}^{2n})$ for $n = 0, 1, 2$, as a function of the scale k/k_{uv} . As shown in Fig. 1, each unscaled component shares a similar shape in the infrared regime $k \lesssim k_{\text{uv}}$, and exhibits a rapid decline in the ultraviolet regime $k \gtrsim k_{\text{uv}}$, which results from the unphysical cutoff $\Theta(k_{\text{uv}} - k)$ in $\Delta_{\mathcal{S}_g}^2$. With the exception of

the unphysical ultraviolet regime, the unscaled components for $n = 0$ and $n = 1$ demonstrate comparable magnitudes, both surpassing the unscaled component for $n = 2$. It indicates that within the regime of $\mathcal{A}_{S,\text{iso}} F_{\text{NL,iso}}^2 < 1$, the non-Gaussian contribution would enhance $\bar{\Omega}_{\text{gw,e}}$ of isocurvature-induced GWs, but not significantly. In particular, the non-Gaussian contributions are almost negligible for $\mathcal{A}_{S,\text{iso}} F_{\text{NL,iso}}^2 \lesssim \mathcal{O}(0.1)$. These results are different from those of SIGWs, where the non-Gaussianity of curvature perturbations could notably change the energy-density fraction spectrum of SIGWs [37–61].

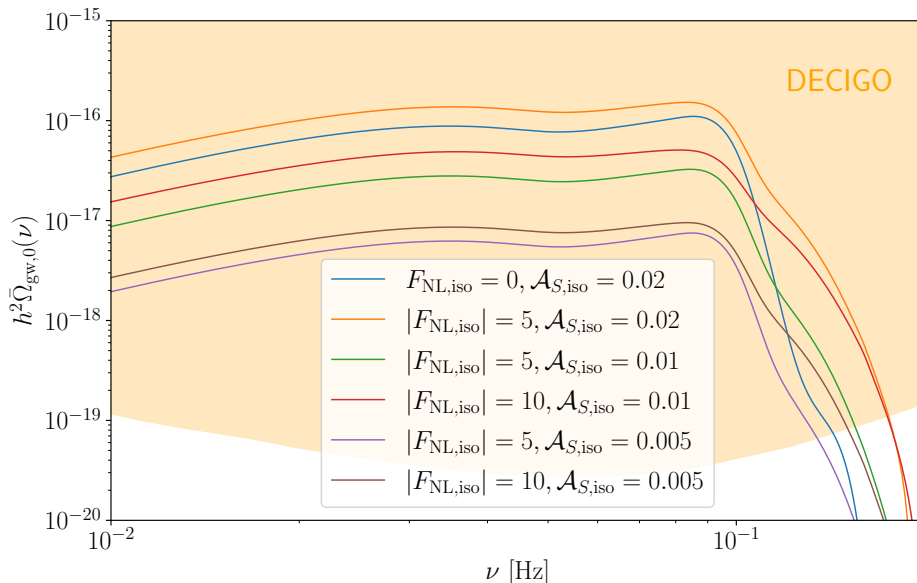


Figure 2. The present-day physical energy-density fraction spectrum $h^2 \bar{\Omega}_{\text{gw},0}$ as a function of the GW frequency ν for different values of $|F_{\text{NL,iso}}|$ and $\mathcal{A}_{S,\text{iso}}$. We compare $h^2 \bar{\Omega}_{\text{gw},0}$ with the sensitivity region of DECIGO (orange shaded area) [82, 83]. Other parameters are set as $k_{\text{uv}}/k_{\text{eeq}} = 50$ and $\nu_{\text{uv}} = k_{\text{uv}}/(2\pi) = 0.1$ Hz.

Regarding observations, we consider the present-day physical energy-density fraction spectrum, denoted as $h^2 \bar{\Omega}_{\text{gw},0}(\nu)$, i.e.,

$$h^2 \bar{\Omega}_{\text{gw},0}(\nu) \simeq h^2 \Omega_{\text{rad},0} \bar{\Omega}_{\text{gw,e}}(k) \Big|_{k=2\pi\nu}, \quad (3.16)$$

where ν denotes the GW frequency, $h^2 \Omega_{\text{rad},0} \simeq 4.18 \times 10^{-5}$ is the present-day physical density fraction of radiation with h being the dimensionless Hubble constant [75]. The explicit expression in Eq. (3.16) may be influenced by the following two factors. Firstly, the change in the effective number of relativistic degrees of freedom in the Universe contributes a factor of $(g_{*\rho,e}/g_{*\rho,0}) (g_{*s,e}/g_{*s,0})^{-4/3}$, where $g_{*\rho}$ (or g_{*s}) represents the effective number of relativistic degrees of freedom in the energy density (or entropy). This factor is model-dependent and is anticipated to be of $\mathcal{O}(1)$. Secondly, the decay of solitons into relativistic particles could introduce additional radiation components into the Universe, potentially affecting the result in Eq. (3.16). Since we have assumed that the solitons decay at $\eta \simeq \eta_{\text{eeq}}$ in order to avoid the soliton domination, this effect is expected to contribute only a correction factor of $\mathcal{O}(1)$. We plot Fig. 2 to illustrate the frequency dependence of $h^2 \bar{\Omega}_{\text{gw},0}(\nu)$ for different values of $|F_{\text{NL,iso}}|$ and $\mathcal{A}_{S,\text{iso}}$. It is shown that $\bar{\Omega}_{\text{gw},0}$ exhibits a double-peak structure at $\nu \lesssim \nu_{\text{uv}}$ and sharply declines at $\nu \gtrsim \nu_{\text{uv}}$. The amplitude of $\bar{\Omega}_{\text{gw},0}$ is mainly determined by $\mathcal{A}_{S,\text{iso}}$ with

$\bar{\Omega}_{\text{gw},0} \propto \mathcal{A}_{S,\text{iso}}^2$. For $\mathcal{O}(0.1) \lesssim \mathcal{A}_{S,\text{iso}} F_{\text{NL,iso}}^2 < 1$, $\bar{\Omega}_{\text{gw},0}$ could also be enhanced due to the contribution of non-Gaussianity. Moreover, we also compare $h^2 \bar{\Omega}_{\text{gw},0}(\nu)$ with the sensitivity curve of Deci-hertz Interferometer Gravitational wave Observatory (DECIGO) [82, 83]. The isocurvature-induced GWs involved in our work are potentially detectable for DECIGO in future.

Our findings regarding the effects of non-Gaussianity on $\bar{\Omega}_{\text{gw}}$ of isocurvature-induced GWs have the following implications. Firstly, we demonstrate that the shape of $\bar{\Omega}_{\text{gw},0}$ for the ‘‘universal GWs’’ from solitons, as discussed in Ref. [4], remains nearly unchanged in the perturbative regime, regardless of the presence of non-Gaussianity in soliton isocurvature perturbations. Consequently, our research broadens the applicable condition for such ‘‘universal GWs’’ as a distinct signal for detecting solitons. Secondly, since the effects of non-Gaussianity on $\bar{\Omega}_{\text{gw},0}$ are highly degenerate, relying solely on $\bar{\Omega}_{\text{gw},0}$ for measurements of non-Gaussianity is unlikely to be effective. Therefore, it is quite imperative to establish novel observables in the isocurvature-induced GWs to detect the non-Gaussianity. This provides strong motivations for our subsequent exploration of the anisotropies in the isocurvature-induced GWs.

4 Anisotropies of isocurvature-induced GWs

In this section, we move on to study the inhomogeneities in the energy density of isocurvature-induced GWs, which are mapping as the anisotropies over the skymap. The non-Gaussianity indicates the interaction between large- and small-scale isocurvature perturbations, which can redistribute the energy density of GWs and lead to inhomogeneities at superhorizon scales. These inhomogeneities, combined with the propagation effects of GWs [64, 76, 77, 84], ultimately give rise to the observed anisotropies of GWs. We will obtain the (reduced) angular power spectrum as an observable characterizing these anisotropies.

4.1 Reduced angular power spectrum

The anisotropies in isocurvature-induced GWs are related to the density contrast of GWs at the emission time, namely, $\delta_{\text{gw},e}(\mathbf{k}) = \delta_{\text{gw}}(\eta_e, \mathbf{x}_e, \mathbf{k})$. Since the angle subtended by the horizon at η_e is extremely small compared to the angular resolution of GW detectors, the GW signal along the line of sight is actually an average over a large number of such horizons. The small-scale $\delta_{\text{gw},e}$ would be averaged to zero, and thus makes no contribution to observed anisotropies. Therefore, the anisotropies of GWs originate solely from large-scale $\delta_{\text{gw},e}$. This large-scale $\delta_{\text{gw},e}$ could be generated by the non-Gaussianity in \mathcal{S} , which introduces the coupling between \mathcal{S}_{gS} and \mathcal{S}_{gL} . As aforementioned, the subscripts S and L , respectively, stand for short- and long-wavelength modes. The GWs induced by \mathcal{S}_S can be spatially modulated at large scales by \mathcal{S}_{gL} , through the non-linear term $\mathcal{S}_S \sim F_{\text{NL,iso}} \mathcal{S}_{gS} \mathcal{S}_{gL}$ in Eq. (2.3). To illustrate the above picture, we expand $\rho_{\text{gw}} \sim \langle \mathcal{S}^4 \rangle$ to the linear order of \mathcal{S}_{gL} , i.e.,

$$\langle \mathcal{S}^4 \rangle = \langle \mathcal{S}_S^4 \rangle + \mathcal{O}(\mathcal{S}_{gL}) F_{\text{NL,iso}} \langle \mathcal{S}_S^3 \mathcal{S}_{gS} \rangle + \mathcal{O}(\mathcal{S}_{gL}^2). \quad (4.1)$$

On the right-hand side of Eq. (4.1), the first term is corresponding to $\bar{\Omega}_{\text{gw},e}$, while the second term gives the leading order of the large-scale density contrast due to the spatial modulation of \mathcal{S}_{gL} , namely $\delta_{\text{gw},e} \sim F_{\text{NL,iso}} \langle \mathcal{S}_S^3 \mathcal{S}_{gS} \rangle \mathcal{S}_{gL}$. Employing the diagrammatic approach akin to the study of SIGWs [42, 43, 62], the explicit expression of $\delta_{\text{gw},e}$ is showed as

$$\delta_{\text{gw},e}(\mathbf{k}) = F_{\text{NL,iso}} \frac{\bar{\Omega}_{\text{ng},e}(k)}{\bar{\Omega}_{\text{gw},e}(k)} \int \frac{d^3 \mathbf{q}}{(2\pi)^{3/2}} e^{i\mathbf{q} \cdot \mathbf{x}_e} \mathcal{S}_{gL}(\mathbf{q}), \quad (4.2)$$

where $\bar{\Omega}_{\text{ng,e}}$ is defined as

$$\bar{\Omega}_{\text{ng,e}}(k) = 2^3 \bar{\Omega}_{\text{gw,e}}^G(k) + 2^2 \bar{\Omega}_{\text{gw,e}}^H(k) + 2^2 \bar{\Omega}_{\text{gw,e}}^C(k) + 2^2 \bar{\Omega}_{\text{gw,e}}^Z(k) . \quad (4.3)$$

Additionally, the $\mathcal{O}(\mathcal{S}_{gL}^2)$ term in Eq. (4.1) can be safely neglected when considering $\mathcal{A}_{L,\text{iso}} \ll \mathcal{A}_{S,\text{iso}}$ in our present work.

In order to get the present-day density contrast $\delta_{\text{gw},0}(\mathbf{k}) = \delta_{\text{gw}}(\eta_0, \mathbf{x}_0, \mathbf{k})$ for an observer located at (η_0, \mathbf{x}_0) , we solve the Boltzmann equation governing the evolution of GWs, following a line-of-sight approach [76, 77, 84]. The $\delta_{\text{gw},0}$ consists of $\delta_{\text{gw,e}}$ and propagation effects in a way that is similar to the study of SIGWs [42–46, 62–67]. It is given by

$$\delta_{\text{gw},0}(\mathbf{k}) = \delta_{\text{gw,e}}(\mathbf{k}) + [4 - n_{\text{gw},0}(k)] \Phi(\eta_e, \mathbf{x}_e) + \dots , \quad (4.4)$$

where the second term on the right-hand side arises from gravitational redshift or blueshift caused by cosmological scalar perturbations, known as the Sachs-Wolfe (SW) effect [85], and the ellipsis could include other propagation effects such as the integrated Sachs-Wolfe (ISW) effect [85], which is usually expected to be negligible (e.g., see Ref. [62] for the case of SIGWs). Nonetheless, we can take these effects into account if necessary [64, 69, 86]. In Eq. (4.4), the spectral index $n_{\text{gw},0}(k)$ is defined as

$$n_{\text{gw},0}(k) = \left. \frac{\partial \ln \bar{\Omega}_{\text{gw},0}(\nu)}{\partial \ln \nu} \right|_{k=2\pi\nu} \simeq \frac{\partial \ln \bar{\Omega}_{\text{gw,e}}(k)}{\partial \ln k} , \quad (4.5)$$

and the large-scale scalar perturbation $\Phi(\eta_e, \mathbf{x}_e)$ is approximately given by large-scale curvature perturbations, i.e.,

$$\Phi(\eta_e, \mathbf{x}_e) \simeq \frac{3}{5} \int \frac{d^3 \mathbf{q}}{(2\pi)^{3/2}} e^{i\mathbf{q}\cdot\mathbf{x}_e} \zeta_L(\mathbf{q}) , \quad (4.6)$$

where we neglect contributions of large-scale isocurvature perturbations due to $\mathcal{A}_{L,\text{iso}} \ll \mathcal{A}_{\text{ad}}$.

Assuming the cosmological principle, we define the reduced angular power spectrum to describe the anisotropies of GWs, i.e.,

$$\langle \delta_{\text{gw},0,\ell_1 m_1}(k_1) \delta_{\text{gw},0,\ell_2 m_2}^*(k_2) \rangle = \delta_{\ell_1 \ell_2} \delta_{m_1 m_2} \tilde{C}_\ell(k_1, k_2) , \quad (4.7)$$

which can be evaluated within the same frequency band (i.e., $k_1 = k_2$) or across different frequency bands (i.e., $k_1 \neq k_2$). Here, $\delta_{\text{gw},0,\ell m}$ denotes the coefficient in the spherical harmonic expansion of $\delta_{\text{gw},0}$, namely,

$$\delta_{\text{gw},0}(\mathbf{k}) = \sum_{\ell m} \delta_{\text{gw},0,\ell m}(k) Y_{\ell m}(\hat{\mathbf{k}}) . \quad (4.8)$$

Analogous to calculations in Refs. [42–44, 62–64, 76, 77], the reduced angular power spectrum of isocurvature-induced GWs can be derived from Eqs. (4.2–4.8). It is given by

$$\tilde{C}_\ell(k_1, k_2) = \frac{2\pi \mathcal{A}_{\text{ad}}}{\ell(\ell+1)} \left\{ \beta F_{\text{NL,iso}}^2 \frac{\bar{\Omega}_{\text{ng,e}}(k_1) \bar{\Omega}_{\text{ng,e}}(k_2)}{\bar{\Omega}_{\text{gw,e}}(k_1) \bar{\Omega}_{\text{gw,e}}(k_2)} + \frac{9}{25} [4 - n_{\text{gw},0}(k_1)] [4 - n_{\text{gw},0}(k_2)] \right\} , \quad (4.9)$$

where we use the large-scale correlations, i.e., $\langle \zeta_L \zeta_L \rangle \sim \mathcal{A}_{\text{ad}}$, $\langle \mathcal{S}_{gL} \mathcal{S}_{gL} \rangle \sim \mathcal{A}_{L,\text{iso}} = \beta \mathcal{A}_{\text{ad}}$, and $\langle \zeta_L \mathcal{S}_{gL} \rangle = 0$. The first and second terms in the bracket of Eq. (4.9) correspond to $\delta_{\text{gw,e}}$ and the SW effect term, respectively.

Eq. (4.9) is one of the key results of our work. It is essential to compare Eq. (4.9) with the reduced angular power spectrum of SIGWs (e.g., see Eq. (5.16) in Ref. [42]), with the main differences emphasized as follows. Firstly, the expression for \tilde{C}_ℓ in Eq. (4.9) introduces a novel parameter β . It is easily understood, because two $\delta_{\text{gw},0}$ with large spatial separation are correlated by \mathcal{S}_{gL} for the case of isocurvature-induced GWs, while by ζ_L for the case of SIGWs. Secondly, in Eq. (4.9), the cross term between $\delta_{\text{gw},e}$ and the SW effect does not exist, different from the case of SIGWs. This is because we have $\delta_{\text{gw},e} \propto \mathcal{S}_{gL}$ and $(4 - n_{\text{gw}})\Phi \propto \zeta_L$ in Eq. (4.4), leading to the vanishing correlation between them, i.e., $\langle \zeta_L \mathcal{S}_{gL} \rangle = 0$. This results in some unique features in the anisotropies of isocurvature-induced GWs, as will be demonstrated below.

4.2 Numerical results

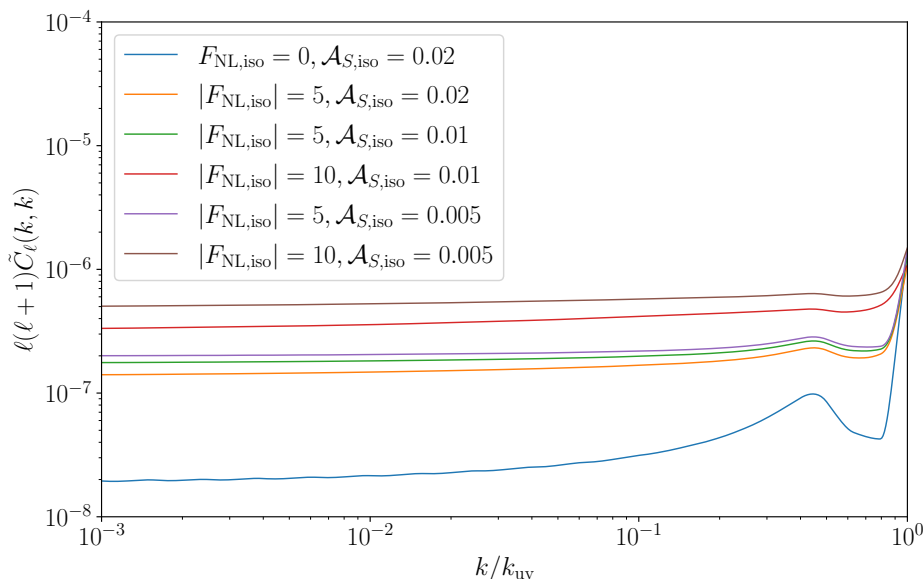


Figure 3. Reduced angular power spectrum $\ell(\ell+1)\tilde{C}_\ell$ versus the GW wavenumber k for various values of $|F_{\text{NL,iso}}|$ and $\mathcal{A}_{S,\text{iso}}$. We set $\beta = 10^{-2}$.

In Fig. 3, we illustrate the k -dependence of $\ell(\ell+1)\tilde{C}_\ell(k, k)$ for various values of $|F_{\text{NL,iso}}|$ and $\mathcal{A}_{S,\text{iso}}$. It is illustrated that $\ell(\ell+1)\tilde{C}_\ell$ is primarily influenced by $|F_{\text{NL,iso}}|$ but shows little sensitivity to $\mathcal{A}_{S,\text{iso}}$. The anisotropies can be boosted by approximately two orders of magnitude due to non-Gaussianity, as compared to the Gaussian cases. Therefore, the detection of the anisotropies could be helpful to break the high degeneracy of $|F_{\text{NL,iso}}|$ on $\bar{\Omega}_{\text{gw}}$. We note that the non-linearity parameter $F_{\text{NL,iso}}$ exhibits a strict sign degeneracy in $\ell(\ell+1)\tilde{C}_\ell$ due to the absence of the cross term between $\delta_{\text{gw},e}$ and the SW effect in Eq. (4.9), different from the case of SIGWs. Additionally, the sharp increase in $\ell(\ell+1)\tilde{C}_\ell$ at $k \simeq k_{\text{uv}}$ is attributed to the pronounced SW effect, which arises from the rapid decrease in $\bar{\Omega}_{\text{gw}}$ at $k \simeq k_{\text{uv}}$ due to the unphysical cutoff in $\Delta_{S_g}^2$.

Multiplying by the energy-density fraction spectrum, the reduced angular power spectrum is further reformulated as the angular power spectrum, i.e.,

$$C_\ell(\nu_1, \nu_2) = \frac{\bar{\Omega}_{\text{gw},0}(\nu_1)}{4\pi} \frac{\bar{\Omega}_{\text{gw},0}(\nu_2)}{4\pi} \tilde{C}_\ell(k_1, k_2) \Big|_{k_1=2\pi\nu_1, k_2=2\pi\nu_2}. \quad (4.10)$$

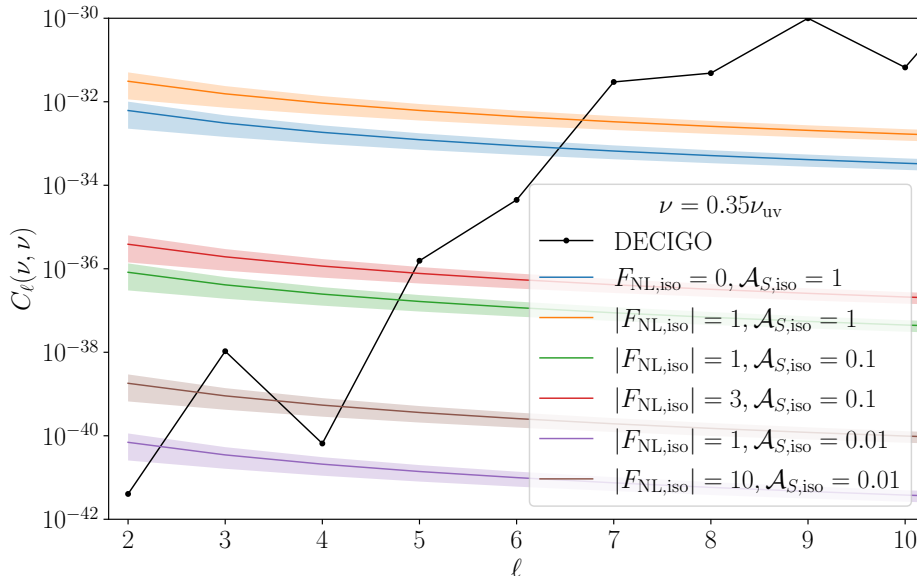


Figure 4. Multipole dependence of the angular power spectrum $C_\ell(\nu, \nu)$ for different values of $|F_{\text{NL,iso}}|$ and $\mathcal{A}_{S,\text{iso}}$. Shaded regions represent the uncertainties (68% confidence level) due to the cosmic variance, i.e., $\Delta C_\ell/C_\ell = \sqrt{2/(2\ell+1)}$. We compare $C_\ell(\nu, \nu)$ to the noise angular power spectrum of DECIGO [87], with a frequency ν aligning with the optimal sensitivity frequency. Other parameters are set as $\beta = 10^{-2}$ and $k_{\text{uv}}/k_{\text{eeq}} = 20$.

In Fig. 4, we depict the multipole dependence of $C_\ell(\nu, \nu)$ for different values of $|F_{\text{NL,iso}}|$ and $\mathcal{A}_{S,\text{iso}}$, with $\nu = 0.35 \nu_{\text{uv}}$ positioned close to the left peak of $\bar{\Omega}_{\text{gw}}$. Similar to the multipole dependence of C_ℓ of SIGWs, the multipole dependence of C_ℓ of isocurvature-induced GWs also follows $C_\ell \propto [\ell(\ell+1)]^{-1}$, which is instrumental in differentiating them from other sources of GWs and astrophysical foregrounds. Increasing $|F_{\text{NL,iso}}|$ and $\mathcal{A}_{S,\text{iso}}$ could lead to an increase of C_ℓ . Comparing $C_\ell(\nu, \nu)$ with the optimal sensitivity of DECIGO [87], as shown in Fig. 4, we infer that only for large values of $\mathcal{A}_{S,\text{iso}}$, e.g., $\mathcal{A}_{S,\text{iso}} \gtrsim \mathcal{O}(0.1)$, the anisotropies of isocurvature-induced GWs are potentially observed at low- ℓ multipoles by DECIGO.

In contrast to the study of the CMB, for which only the correlation between the same frequency band is considered due to the blackbody nature of the CMB, we define the cross-correlation between different frequency bands of isocurvature-induced GWs as

$$r_\ell(k_1, k_2) = \frac{\tilde{C}_\ell(k_1, k_2)}{\sqrt{\tilde{C}_\ell(k_1, k_1)\tilde{C}_\ell(k_2, k_2)}}. \quad (4.11)$$

In Fig. 5, we visualize it for different values of $|F_{\text{NL,iso}}|$ and $\mathcal{A}_{S,\text{iso}}$. In the regimes of $(k_1 \lesssim k_{\text{uv}}, k_2 \lesssim k_{\text{uv}})$ and $(k_1 \gtrsim k_{\text{uv}}, k_2 \gtrsim k_{\text{uv}})$, we have $r_\ell(k_1, k_2) \simeq 1$. However, in the regimes of $(k_1 \gtrsim k_{\text{uv}}, k_2 \lesssim k_{\text{uv}})$ and $(k_1 \lesssim k_{\text{uv}}, k_2 \gtrsim k_{\text{uv}})$, we find $r_\ell(k_1, k_2) < 1$, indicating that the anisotropies for different frequency bands are not fully correlated. Our analysis also indicates that $r_\ell(k_1, k_2)$ can be affected by $|F_{\text{NL,iso}}|$. In the case of Gaussianity, we consistently have $r_\ell(k_1, k_2) = 1$. However, $r_\ell(k_1, k_2)$ decreases as $|F_{\text{NL,iso}}|$ increases in the regimes of $(k_1 \gtrsim k_{\text{uv}}, k_2 \lesssim k_{\text{uv}})$ and $(k_1 \lesssim k_{\text{uv}}, k_2 \gtrsim k_{\text{uv}})$. Therefore, $r_\ell(k_1, k_2)$ could also be a probe to discern the value of $|F_{\text{NL,iso}}|$.

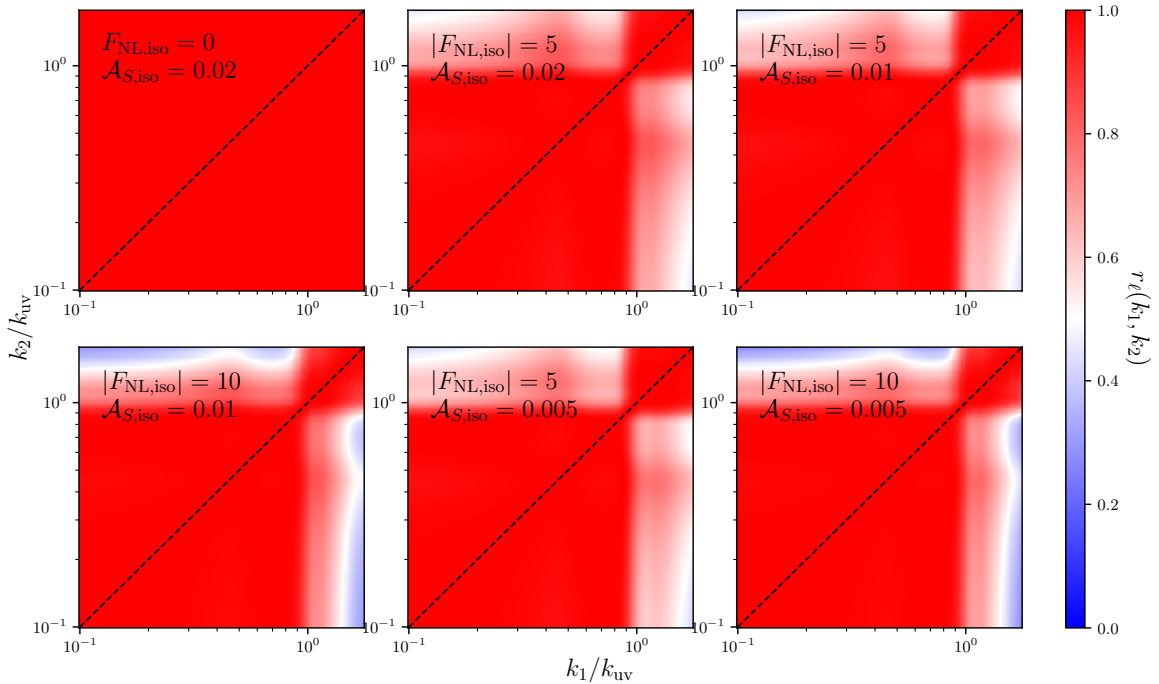


Figure 5. Cross-correlation factor $r_\ell(k_1, k_2)$ with respect to the GW wavenumber band for different values of $|F_{\text{NL,iso}}|$ and $\mathcal{A}_{S,\text{iso}}$. In each panel, the dashed line refers to $k_1 = k_2$. We use the same sets of model parameters as those of Fig. 2 and set $\beta = 10^{-2}$ for all cases.

5 Conclusions and discussion

In this study, we have investigated the GWs induced by the non-Gaussian soliton isocurvature perturbations, encompassing both their isotropic background and anisotropies. As an important result for the isotropic background, we found that the non-Gaussianity would not significantly affect both the amplitude and shape of the energy-density fraction spectrum in the perturbative regime. This result indicates that the “universal GWs” still serves as a unique signal to identify solitons, even if the soliton isocurvature perturbations are non-Gaussian. The insensitive dependence of the energy-density fraction spectrum on $|F_{\text{NL,iso}}|$ could bring a significant challenge to measure the non-Gaussianity. To address this challenge, we provided the first analysis of the anisotropies of isocurvature-induced GWs, accounting for both $\delta_{\text{gw,e}}$ and the propagation effects. As another key result in this work, the (reduced) angular power spectrum, as demonstrated by Eq. (4.9), could serve as a powerful probe of the non-Gaussianity in isocurvature perturbations. It highlights the significant role of this non-Gaussianity in enhancing anisotropies in isocurvature-induced GWs, breaking the degeneracies between $|F_{\text{NL,iso}}|$ and other model parameters such as $\mathcal{A}_{S,\text{iso}}$. The expression of the (reduced) angular power spectrum also showcases the intrinsic differences between the anisotropies of isocurvature-induced GWs and those of SIGWs. The isotropic background and anisotropies of isocurvature-induced GWs can provide novel probes and signatures for diverse cosmological models related to soliton formation, enriching our understanding of the early Universe.

As a related work, Ref. [24] discussed the effects of non-Gaussianity on the GWs induced by dark matter isocurvature perturbations. The authors estimate that the non-Gaussianity

may significantly enhance $\Omega_{\text{gw},0}$, which seems different from our result. However, these two are not contradictory in essence. In fact, the differences mainly come from the following two aspects. (a) In Ref. [24], GWs are produced in standard radiation-matter Universe with a suppression of power-law $(k/k_{\text{eq}})^{-4}$ on $\bar{\Omega}_{\text{gw},e}(k)$, where $k_{\text{eq}} \sim 0.01 \text{ Mpc}^{-1}$ is the mode reentering the horizon at standard radiation-matter equality. To generate detectable GWs within the frequency band of GW detectors, $\mathcal{A}_{S,\text{iso}}$ needs to be much larger than unity to overcome the suppression factor. However, in our paper, the corresponding suppression factor is $(k/k_{\text{eeq}})^{-4}$ for an early radiation-soliton Universe. We consider the case $\mathcal{A}_{S,\text{iso}} \lesssim 1$, which is enough to generate detectable GWs. (b) In Ref. [24], the GW sources are highly skewed non-Gaussian \mathcal{S} that can not be parameterized as Eq. (2.3). Whereas in our present work, we consider the non-Gaussian \mathcal{S} in the form of Eq. (2.3).

In this work, we have assumed that solitons decay before they dominate the early Universe. If solitons could dominate the early Universe, their decay might introduce additional relativistic degrees of freedom and also change the energy density of radiation, depending on specific models and the duration of soliton domination. These effects would notably suppress the amplitudes of $\bar{\Omega}_{\text{gw},0}$ and C_ℓ , making them more challenging to be observed. However, other main results presented in this paper are expected to remain unchanged.

We may further investigate cross-correlations between the isocurvature-induced GWs with the CMB temperature anisotropies and polarization. Recent studies have explored the cross-correlations between SIGWs and the CMB [64, 68, 69]. The cross-correlations could be significant since the anisotropies of SIGWs and the CMB share the same origin, i.e., curvature perturbations. In contrast, the isocurvature-induced GWs exhibit minimal cross-correlations with the CMB, since their anisotropies mainly originate from the isocurvature perturbations (with other effects such as the SW effect being subdominant), which are expected not to correlate with the curvature perturbations. These distinctions reveal that the cross-correlations between the GW signal and the CMB could serve as crucial observable to identify the isocurvature-induced GWs.

Our study of isocurvature-induced GWs may provide important implications for primordial black holes (PBHs), which are a promising candidate for dark matter. If solitons temporarily dominate the early Universe before their decay, the overdensities caused by their number density fluctuations could be the seeds for PBH formation [88–92], accompanied by GWs induced by soliton isocurvature perturbations. For comparison, PBHs could also be produced through the gravitational collapse of enhanced small-scale curvature perturbations [93], accompanied by the production of SIGWs. The above two mechanisms of PBH formation are potentially distinguishable via identifying the corresponding GW signals, e.g., through their cross-correlations with the CMB. Furthermore, the presence of non-Gaussianity in soliton isocurvature perturbations may modify the abundance of PBHs and also lead to a clustering of PBHs. However, this intriguing topic is beyond the scope of our current study. Hence, we leave it to future works.

Acknowledgments

S.W. would like to express his gratitude to Xian Gao and Jiarui Sun for their warm hospitality during the final stage of this work, which was conducted during a visit to the Sun Yat-sen University. This work is supported by the National Key R&D Program of China No. 2023YFC2206403 and the National Natural Science Foundation of China (Grant No. 12175243).

A Formulas for the energy-density fraction spectrum

In this Appendix, we summarize the formulas for $\bar{\Omega}_{\text{gw},e}^X$ ($X = G, H, C, Z, R, P, N$) in Eq. (3.15) as forms suitable for numerical integration. Similar results for the case of SIGWs can be found in Refs. [37–44]. To be specific, the $\bar{\Omega}_{\text{gw},e}^{(0)}$ component is given by of $\bar{\Omega}_{\text{gw},e}^G$, namely,

$$\bar{\Omega}_{\text{gw},e}^G(k) = \frac{1}{3} \int_0^\infty dt_1 \int_{-1}^1 ds_1 \overline{J^2(u_1, v_1, \kappa, x \rightarrow \infty)} \frac{1}{(u_1 v_1)^2} \Delta_{\mathcal{S}_g}^2(v_1 k) \Delta_{\mathcal{S}_g}^2(u_1 k). \quad (\text{A.1})$$

The $\bar{\Omega}_{\text{gw},e}^{(1)}$ component consists of $\bar{\Omega}_{\text{gw},e}^H$, $\bar{\Omega}_{\text{gw},e}^C$, and $\bar{\Omega}_{\text{gw},e}^Z$, namely,

$$\begin{aligned} \bar{\Omega}_{\text{gw},e}^H(k) &= \frac{1}{3} F_{\text{NL,iso}}^2 \prod_{i=1}^2 \left[\int_0^\infty dt_i \int_{-1}^1 ds_i \right] \overline{J^2(u_1, v_1, \kappa, x \rightarrow \infty)} \frac{1}{(u_1 v_1 u_2 v_2)^2} \\ &\quad \times \Delta_{\mathcal{S}_g}^2(v_1 v_2 k) \Delta_{\mathcal{S}_g}^2(u_1 k) \Delta_{\mathcal{S}_g}^2(v_1 u_2 k), \end{aligned} \quad (\text{A.2})$$

$$\begin{aligned} \bar{\Omega}_{\text{gw},e}^C(k) &= \frac{1}{3\pi} F_{\text{NL,iso}}^2 \prod_{i=1}^2 \left[\int_0^\infty dt_i \int_{-1}^1 ds_i v_i u_i \right] \int_0^{2\pi} d\varphi_{12} \cos 2\varphi_{12} \\ &\quad \times \overline{J(u_1, v_1, \kappa, x \rightarrow \infty) J(u_2, v_2, \kappa, x \rightarrow \infty)} \\ &\quad \times \frac{\Delta_{\mathcal{S}_g}^2(v_2 k)}{v_2^3} \frac{\Delta_{\mathcal{S}_g}^2(u_2 k)}{u_2^3} \frac{\Delta_{\mathcal{S}_g}^2(w_{12} k)}{w_{12}^3}, \end{aligned} \quad (\text{A.3})$$

$$\begin{aligned} \bar{\Omega}_{\text{gw},e}^Z(k) &= \frac{1}{3\pi} F_{\text{NL,iso}}^2 \prod_{i=1}^2 \left[\int_0^\infty dt_i \int_{-1}^1 ds_i v_i u_i \right] \int_0^{2\pi} d\varphi_{12} \cos 2\varphi_{12} \\ &\quad \times \overline{J(u_1, v_1, \kappa, x \rightarrow \infty) J(u_2, v_2, \kappa, x \rightarrow \infty)} \\ &\quad \times \frac{\Delta_{\mathcal{S}_g}^2(v_2 k)}{v_2^3} \frac{\Delta_{\mathcal{S}_g}^2(u_1 k)}{u_1^3} \frac{\Delta_{\mathcal{S}_g}^2(w_{12} k)}{w_{12}^3}. \end{aligned} \quad (\text{A.4})$$

The $\bar{\Omega}_{\text{gw},e}^{(2)}$ component consists of $\bar{\Omega}_{\text{gw},e}^R$, $\bar{\Omega}_{\text{gw},e}^P$, and $\bar{\Omega}_{\text{gw},e}^N$, namely,

$$\begin{aligned} \bar{\Omega}_{\text{gw},e}^R(k) &= \frac{1}{12} F_{\text{NL,iso}}^4 \prod_{i=1}^3 \left[\int_0^\infty dt_i \int_{-1}^1 ds_i \right] \overline{J^2(u_1, v_1, \kappa, x \rightarrow \infty)} \frac{1}{(u_1 v_1 u_2 v_2 u_3 v_3)^2} \\ &\quad \times \Delta_{\mathcal{S}_g}^2(v_1 v_2 k) \Delta_{\mathcal{S}_g}^2(v_1 u_2 k) \Delta_{\mathcal{S}_g}^2(u_1 v_3 k) \Delta_{\mathcal{S}_g}^2(u_1 u_3 k), \end{aligned} \quad (\text{A.5})$$

$$\begin{aligned} \bar{\Omega}_{\text{gw},e}^P(k) &= \frac{1}{24\pi^2} F_{\text{NL,iso}}^4 \prod_{i=1}^3 \left[\int_0^\infty dt_i \int_{-1}^1 ds_i v_i u_i \right] \int_0^{2\pi} d\varphi_{12} d\varphi_{23} \cos 2\varphi_{12} \\ &\quad \times \overline{J(u_1, v_1, \kappa, x \rightarrow \infty) J(u_2, v_2, \kappa, x \rightarrow \infty)} \\ &\quad \times \frac{\Delta_{\mathcal{S}_g}^2(v_3 k)}{v_3^3} \frac{\Delta_{\mathcal{S}_g}^2(u_3 k)}{u_3^3} \frac{\Delta_{\mathcal{S}_g}^2(w_{13} k)}{w_{13}^3} \frac{\Delta_{\mathcal{S}_g}^2(w_{23} k)}{w_{23}^3}, \end{aligned} \quad (\text{A.6})$$

$$\begin{aligned} \bar{\Omega}_{\text{gw},e}^N(k) &= \frac{1}{24\pi^2} F_{\text{NL,iso}}^4 \prod_{i=1}^3 \left[\int_0^\infty dt_i \int_{-1}^1 ds_i v_i u_i \right] \int_0^{2\pi} d\varphi_{12} d\varphi_{23} \cos 2\varphi_{12} \\ &\quad \times \overline{J(u_1, v_1, \kappa, x \rightarrow \infty) J(u_2, v_2, \kappa, x \rightarrow \infty)} \end{aligned}$$

$$\times \frac{\Delta_{\mathcal{S}_g}^2(u_3 k)}{u_3^3} \frac{\Delta_{\mathcal{S}_g}^2(w_{13} k)}{w_{13}^3} \frac{\Delta_{\mathcal{S}_g}^2(w_{23} k)}{w_{23}^3} \frac{\Delta_{\mathcal{S}_g}^2(w_{123} k)}{w_{123}^3}. \quad (\text{A.7})$$

In Eqs. (A.1-A.7), we have introduced a new function $J(u_i, v_i, \kappa, x)$, defined as

$$J(u_i, v_i, \kappa, x) = \frac{x}{8} [(v_i + u_i)^2 - 1] [1 - (v_i - u_i)^2] \hat{I}(u_i, v_i, \kappa, x), \quad (\text{A.8})$$

where we have used $\kappa = k/k_{\text{ceq}}$ and $x = k\eta$, and $\hat{I}(u_i, v_i, \kappa, x)$ has been given in Eq. (3.11). Additionally, we have introduced the following new notations

$$s_i = u_i - v_i, \quad (\text{A.9})$$

$$t_i = u_i + v_i - 1, \quad (\text{A.10})$$

$$y_{ij} = \frac{\cos \varphi_{ij}}{4} \sqrt{t_i(t_i + 2)(1 - s_i^2)t_j(t_j + 2)(1 - s_j^2)} + \frac{1}{4} [1 - s_i(t_i + 1)][1 - s_j(t_j + 1)], \quad (\text{A.11})$$

$$w_{ij} = \sqrt{v_i^2 + v_j^2 - y_{ij}}, \quad (\text{A.12})$$

$$w_{123} = \sqrt{v_1^2 + v_2^2 + v_3^2 + y_{12} - y_{13} - y_{23}}. \quad (\text{A.13})$$

References

- [1] S.-Y. Zhou, *Non-topological solitons and quasi-solitons*, [2411.16604](#).
- [2] H. Murayama and J. Shu, *Topological Dark Matter*, *Phys. Lett. B* **686** (2010) 162 [[0905.1720](#)].
- [3] PLANCK collaboration, *Planck 2018 results. X. Constraints on inflation*, *Astron. Astrophys.* **641** (2020) A10 [[1807.06211](#)].
- [4] K.D. Lozanov, M. Sasaki and V. Takhistov, *Universal Gravitational Wave Signatures of Cosmological Solitons*, [2304.06709](#).
- [5] J.M. Maldacena, *Non-Gaussian features of primordial fluctuations in single field inflationary models*, *JHEP* **05** (2003) 013 [[astro-ph/0210603](#)].
- [6] N. Bartolo, E. Komatsu, S. Matarrese and A. Riotto, *Non-Gaussianity from inflation: Theory and observations*, *Phys. Rept.* **402** (2004) 103 [[astro-ph/0406398](#)].
- [7] T.J. Allen, B. Grinstein and M.B. Wise, *Nongaussian Density Perturbations in Inflationary Cosmologies*, *Phys. Lett. B* **197** (1987) 66.
- [8] N. Bartolo, S. Matarrese and A. Riotto, *Nongaussianity from inflation*, *Phys. Rev. D* **65** (2002) 103505 [[hep-ph/0112261](#)].
- [9] V. Acquaviva, N. Bartolo, S. Matarrese and A. Riotto, *Second order cosmological perturbations from inflation*, *Nucl. Phys. B* **667** (2003) 119 [[astro-ph/0209156](#)].
- [10] F. Bernardeau and J.-P. Uzan, *NonGaussianity in multifield inflation*, *Phys. Rev. D* **66** (2002) 103506 [[hep-ph/0207295](#)].
- [11] X. Chen, M.-x. Huang, S. Kachru and G. Shiu, *Observational signatures and non-Gaussianities of general single field inflation*, *JCAP* **01** (2007) 002 [[hep-th/0605045](#)].
- [12] X. Gao, T. Kobayashi, M. Shiraishi, M. Yamaguchi, J. Yokoyama and S. Yokoyama, *Full bispectra from primordial scalar and tensor perturbations in the most general single-field inflation model*, *PTEP* **2013** (2013) 053E03 [[1207.0588](#)].

- [13] X. Gao, *Primordial Non-Gaussianities of General Multiple Field Inflation*, *JCAP* **06** (2008) 029 [0804.1055].
- [14] Q.-G. Huang, *Curvaton with Polynomial Potential*, *JCAP* **11** (2008) 005 [0808.1793].
- [15] Q.-G. Huang, *A Geometric description of the non-Gaussianity generated at the end of multi-field inflation*, *JCAP* **06** (2009) 035 [0904.2649].
- [16] Y.-F. Cai, X. Chen, M.H. Namjoo, M. Sasaki, D.-G. Wang and Z. Wang, *Revisiting non-Gaussianity from non-attractor inflation models*, *JCAP* **05** (2018) 012 [1712.09998].
- [17] K.N. Ananda, C. Clarkson and D. Wands, *The Cosmological gravitational wave background from primordial density perturbations*, *Phys. Rev. D* **75** (2007) 123518 [gr-qc/0612013].
- [18] D. Baumann, P.J. Steinhardt, K. Takahashi and K. Ichiki, *Gravitational Wave Spectrum Induced by Primordial Scalar Perturbations*, *Phys. Rev. D* **76** (2007) 084019 [hep-th/0703290].
- [19] S. Mollerach, D. Harari and S. Matarrese, *CMB polarization from secondary vector and tensor modes*, *Phys. Rev. D* **69** (2004) 063002 [astro-ph/0310711].
- [20] H. Assadullahi and D. Wands, *Constraints on primordial density perturbations from induced gravitational waves*, *Phys. Rev. D* **81** (2010) 023527 [0907.4073].
- [21] G. Domènech, *Scalar Induced Gravitational Waves Review*, *Universe* **7** (2021) 398 [2109.01398].
- [22] J.R. Espinosa, D. Racco and A. Riotto, *A Cosmological Signature of the SM Higgs Instability: Gravitational Waves*, *JCAP* **09** (2018) 012 [1804.07732].
- [23] K. Kohri and T. Terada, *Semianalytic calculation of gravitational wave spectrum nonlinearly induced from primordial curvature perturbations*, *Phys. Rev. D* **97** (2018) 123532 [1804.08577].
- [24] G. Domènech, S. Passaglia and S. Renaux-Petel, *Gravitational waves from dark matter isocurvature*, *JCAP* **03** (2022) 023 [2112.10163].
- [25] K.D. Lozanov, S. Pi, M. Sasaki, V. Takhistov and A. Wang, *Axion Universal Gravitational Wave Interpretation of Pulsar Timing Array Data*, 2310.03594.
- [26] G. Domènech, *Cosmological gravitational waves from isocurvature fluctuations*, *AAPPS Bull.* **34** (2024) 4 [2311.02065].
- [27] K.D. Lozanov, M. Sasaki and V. Takhistov, *Universal gravitational waves from interacting and clustered solitons*, *Phys. Lett. B* **848** (2024) 138392 [2309.14193].
- [28] G. Domènech and M. Sasaki, *Probing primordial black hole scenarios with terrestrial gravitational wave detectors*, *Class. Quant. Grav.* **41** (2024) 143001 [2401.07615].
- [29] G. Domènech, *GW Backgrounds associated with PBHs*, 2402.17388.
- [30] Z.-C. Chen and L. Liu, *Can we distinguish the adiabatic fluctuations and isocurvature fluctuations with pulsar timing arrays?*, 2402.16781.
- [31] G. Domènech and J. Tränkle, *From formation to evaporation: Induced gravitational wave probes of the primordial black hole reheating scenario*, 2409.12125.
- [32] C. Yuan, Z.-C. Chen and L. Liu, *Gauge Dependence of Gravitational Waves Induced by Primordial Isocurvature Fluctuations*, 2410.18996.
- [33] S. Kumar, H. Tai and L.-T. Wang, *Towards a Complete Treatment of Scalar-induced Gravitational Waves with Early Matter Domination*, 2410.17291.
- [34] T. Papanikolaou, X.-C. He, X.-H. Ma, Y.-F. Cai, E.N. Saridakis and M. Sasaki, *New probe of non-Gaussianities with primordial black hole induced gravitational waves*, *Phys. Lett. B* **857** (2024) 138997 [2403.00660].

- [35] I. Dalianis and G.P. Kodaxis, *Reheating in Runaway Inflation Models via the Evaporation of Mini Primordial Black Holes*, *Galaxies* **10** (2022) 31 [2112.15576].
- [36] X.-C. He, Y.-F. Cai, X.-H. Ma, T. Papanikolaou, E.N. Saridakis and M. Sasaki, *Gravitational waves from primordial black hole isocurvature: the effect of non-Gaussianities*, *JCAP* **12** (2024) 039 [2409.11333].
- [37] P. Adshead, K.D. Lozanov and Z.J. Weiner, *Non-Gaussianity and the induced gravitational wave background*, *JCAP* **10** (2021) 080 [2105.01659].
- [38] H.V. Ragavendra, *Accounting for scalar non-Gaussianity in secondary gravitational waves*, *Phys. Rev. D* **105** (2022) 063533 [2108.04193].
- [39] K.T. Abe, R. Inui, Y. Tada and S. Yokoyama, *Primordial black holes and gravitational waves induced by exponential-tailed perturbations*, *JCAP* **05** (2023) 044 [2209.13891].
- [40] C. Yuan, D.-S. Meng and Q.-G. Huang, *Full analysis of the scalar-induced gravitational waves for the curvature perturbation with local-type non-Gaussianities*, *JCAP* **12** (2023) 036 [2308.07155].
- [41] G. Perna, C. Testini, A. Ricciardone and S. Matarrese, *Fully non-Gaussian Scalar-Induced Gravitational Waves*, *JCAP* **05** (2024) 086 [2403.06962].
- [42] J.-P. Li, S. Wang, Z.-C. Zhao and K. Kohri, *Primordial non-Gaussianity f_{NL} and anisotropies in scalar-induced gravitational waves*, *JCAP* **10** (2023) 056 [2305.19950].
- [43] J.-P. Li, S. Wang, Z.-C. Zhao and K. Kohri, *Complete analysis of the background and anisotropies of scalar-induced gravitational waves: primordial non-Gaussianity f_{NL} and g_{NL} considered*, *JCAP* **06** (2024) 039 [2309.07792].
- [44] J.A. Ruiz and J. Rey, *Gravitational waves in ultra-slow-roll and their anisotropy at two loops*, [2410.09014](#).
- [45] S. Wang, Z.-C. Zhao, J.-P. Li and Q.-H. Zhu, *Implications of pulsar timing array data for scalar-induced gravitational waves and primordial black holes: Primordial non-Gaussianity f_{NL} considered*, *Phys. Rev. Res.* **6** (2024) L012060 [2307.00572].
- [46] Y.-H. Yu and S. Wang, *Anisotropies in scalar-induced gravitational-wave background from inflaton-curvaton mixed scenario with sound speed resonance*, *Phys. Rev. D* **109** (2024) 083501 [2310.14606].
- [47] A.J. Iovino, S. Matarrese, G. Perna, A. Ricciardone and A. Riotto, *How Well Do We Know the Scalar-Induced Gravitational Waves?*, [2412.06764](#).
- [48] X.-X. Zeng, R.-G. Cai and S.-J. Wang, *Multiple peaks in gravitational waves induced from primordial curvature perturbations with non-Gaussianity*, *JCAP* **10** (2024) 045 [2406.05034].
- [49] R.-g. Cai, S. Pi and M. Sasaki, *Gravitational Waves Induced by non-Gaussian Scalar Perturbations*, *Phys. Rev. Lett.* **122** (2019) 201101 [1810.11000].
- [50] C. Unal, *Imprints of Primordial Non-Gaussianity on Gravitational Wave Spectrum*, *Phys. Rev. D* **99** (2019) 041301 [1811.09151].
- [51] V. Atal and G. Domènech, *Probing non-Gaussianities with the high frequency tail of induced gravitational waves*, *JCAP* **06** (2021) 001 [2103.01056].
- [52] C. Yuan and Q.-G. Huang, *Gravitational waves induced by the local-type non-Gaussian curvature perturbations*, *Phys. Lett. B* **821** (2021) 136606 [2007.10686].
- [53] Z. Chang, Y.-T. Kuang, D. Wu, J.-Z. Zhou and Q.-H. Zhu, *New constraints on primordial non-Gaussianity from missing two-loop contributions of scalar induced gravitational waves*, *Phys. Rev. D* **109** (2024) L041303 [2311.05102].
- [54] J.-Z. Zhou, Y.-T. Kuang, Z. Chang and H. Lü, *Constraints on primordial black holes from N_{eff} : scalar induced gravitational waves as an extra radiation component*, [2410.10111](#).

- [55] T. Nakama, J. Silk and M. Kamionkowski, *Stochastic gravitational waves associated with the formation of primordial black holes*, *Phys. Rev. D* **95** (2017) 043511 [[1612.06264](#)].
- [56] J. Garcia-Bellido, M. Peloso and C. Unal, *Gravitational Wave signatures of inflationary models from Primordial Black Hole Dark Matter*, *JCAP* **09** (2017) 013 [[1707.02441](#)].
- [57] H.V. Ragavendra, P. Saha, L. Sriramkumar and J. Silk, *Primordial black holes and secondary gravitational waves from ultraslow roll and punctuated inflation*, *Phys. Rev. D* **103** (2021) 083510 [[2008.12202](#)].
- [58] F. Zhang, *Primordial black holes and scalar induced gravitational waves from the E model with a Gauss-Bonnet term*, *Phys. Rev. D* **105** (2022) 063539 [[2112.10516](#)].
- [59] J. Lin, S. Gao, Y. Gong, Y. Lu, Z. Wang and F. Zhang, *Primordial black holes and scalar induced gravitational waves from Higgs inflation with noncanonical kinetic term*, *Phys. Rev. D* **107** (2023) 043517 [[2111.01362](#)].
- [60] L.-Y. Chen, H. Yu and P. Wu, *Primordial non-Gaussianity in inflation with gravitationally enhanced friction*, *Phys. Rev. D* **106** (2022) 063537 [[2210.05201](#)].
- [61] R.-G. Cai, S. Pi, S.-J. Wang and X.-Y. Yang, *Pulsar Timing Array Constraints on the Induced Gravitational Waves*, *JCAP* **10** (2019) 059 [[1907.06372](#)].
- [62] N. Bartolo, D. Bertacca, V. De Luca, G. Franciolini, S. Matarrese, M. Peloso et al., *Gravitational wave anisotropies from primordial black holes*, *JCAP* **02** (2020) 028 [[1909.12619](#)].
- [63] J. Rey, *A consistency relation for induced gravitational wave anisotropies*, [2411.08873](#).
- [64] F. Schulze, L. Valbusa Dall’Armi, J. Lesgourgues, A. Ricciardone, N. Bartolo, D. Bertacca et al., *GW_CLASS: Cosmological Gravitational Wave Background in the cosmic linear anisotropy solving system*, *JCAP* **10** (2023) 025 [[2305.01602](#)].
- [65] LISA COSMOLOGY WORKING GROUP collaboration, *Probing anisotropies of the Stochastic Gravitational Wave Background with LISA*, *JCAP* **11** (2022) 009 [[2201.08782](#)].
- [66] LISA COSMOLOGY WORKING GROUP collaboration, *Cosmology with the Laser Interferometer Space Antenna*, *Living Rev. Rel.* **26** (2023) 5 [[2204.05434](#)].
- [67] A. Malhotra, E. Dimastrogiovanni, G. Domènech, M. Fasiello and G. Tasinato, *New universal property of cosmological gravitational wave anisotropies*, *Phys. Rev. D* **107** (2023) 103502 [[2212.10316](#)].
- [68] E. Dimastrogiovanni, M. Fasiello, A. Malhotra and G. Tasinato, *Enhancing gravitational wave anisotropies with peaked scalar sources*, *JCAP* **01** (2023) 018 [[2205.05644](#)].
- [69] Z.-C. Zhao, S. Wang, J.-P. Li and K. Kohri, *Study of primordial non-Gaussianity f_{NL} and g_{NL} with the cross-correlations between the scalar-induced gravitational waves and the cosmic microwave background*, [2412.02500](#).
- [70] K. Inomata, K. Kohri, T. Nakama and T. Terada, *Enhancement of Gravitational Waves Induced by Scalar Perturbations due to a Sudden Transition from an Early Matter Era to the Radiation Era*, *Phys. Rev. D* **100** (2019) 043532 [[1904.12879](#)].
- [71] K. Inomata, K. Kohri, T. Nakama and T. Terada, *Gravitational Waves Induced by Scalar Perturbations during a Gradual Transition from an Early Matter Era to the Radiation Era*, *JCAP* **10** (2019) 071 [[1904.12878](#)].
- [72] M. Pearce, L. Pearce, G. White and C. Balazs, *Gravitational wave signals from early matter domination: interpolating between fast and slow transitions*, *JCAP* **06** (2024) 021 [[2311.12340](#)].
- [73] H. Kodama and M. Sasaki, *Cosmological Perturbation Theory*, *Prog. Theor. Phys. Suppl.* **78** (1984) 1.

- [74] K.A. Malik and D. Wands, *Cosmological perturbations*, *Phys. Rept.* **475** (2009) 1 [0809.4944].
- [75] PLANCK collaboration, *Planck 2018 results. VI. Cosmological parameters*, *Astron. Astrophys.* **641** (2020) A6 [1807.06209].
- [76] N. Bartolo, D. Bertacca, S. Matarrese, M. Peloso, A. Ricciardone, A. Riotto et al., *Anisotropies and non-Gaussianity of the Cosmological Gravitational Wave Background*, *Phys. Rev. D* **100** (2019) 121501 [1908.00527].
- [77] N. Bartolo, D. Bertacca, S. Matarrese, M. Peloso, A. Ricciardone, A. Riotto et al., *Characterizing the cosmological gravitational wave background: Anisotropies and non-Gaussianity*, *Phys. Rev. D* **102** (2020) 023527 [1912.09433].
- [78] J.-P. Li, S. Wang, Z.-C. Zhao and K. Kohri, *Angular bispectrum and trispectrum of scalar-induced gravitational waves: all contributions from primordial non-Gaussianity f_{NL} and g_{NL}* , *JCAP* **05** (2024) 109 [2403.00238].
- [79] Z. Chang, Y.-T. Kuang, D. Wu and J.-Z. Zhou, *Probing scalar induced gravitational waves with PTA and LISA: the importance of third order correction*, *JCAP* **2024** (2024) 044 [2312.14409].
- [80] J.-Z. Zhou, Y.-T. Kuang, D. Wu, H. Lü and Z. Chang, *Induced gravitational waves for arbitrary higher orders: vertex rules and loop diagrams in cosmological perturbation theory*, [2408.14052](#).
- [81] S. Garcia-Saenz, L. Pinol, S. Renaux-Petel and D. Werth, *No-go theorem for scalar-trispectrum-induced gravitational waves*, *JCAP* **03** (2023) 057 [2207.14267].
- [82] N. Seto, S. Kawamura and T. Nakamura, *Possibility of direct measurement of the acceleration of the universe using 0.1-Hz band laser interferometer gravitational wave antenna in space*, *Phys. Rev. Lett.* **87** (2001) 221103 [astro-ph/0108011].
- [83] S. Kawamura et al., *Current status of space gravitational wave antenna DECIGO and B-DECIGO*, *PTEP* **2021** (2021) 05A105 [2006.13545].
- [84] C.R. Contaldi, *Anisotropies of Gravitational Wave Backgrounds: A Line Of Sight Approach*, *Phys. Lett. B* **771** (2017) 9 [1609.08168].
- [85] R.K. Sachs and A.M. Wolfe, *Perturbations of a cosmological model and angular variations of the microwave background*, *Astrophys. J.* **147** (1967) 73.
- [86] R.-G. Cai, S.-J. Wang, Z.-Y. Yuwen and X.-X. Zeng, *Anisotropies of cosmological gravitational wave backgrounds in non-flat spacetime*, [2410.17721](#).
- [87] M. Braglia and S. Kuroyanagi, *Probing prerecombination physics by the cross-correlation of stochastic gravitational waves and CMB anisotropies*, *Phys. Rev. D* **104** (2021) 123547 [2106.03786].
- [88] E. Cotner and A. Kusenko, *Primordial black holes from supersymmetry in the early universe*, *Phys. Rev. Lett.* **119** (2017) 031103 [1612.02529].
- [89] E. Cotner and A. Kusenko, *Primordial black holes from scalar field evolution in the early universe*, *Phys. Rev. D* **96** (2017) 103002 [1706.09003].
- [90] E. Cotner, A. Kusenko and V. Takhistov, *Primordial Black Holes from Inflaton Fragmentation into Oscillons*, *Phys. Rev. D* **98** (2018) 083513 [1801.03321].
- [91] E. Cotner, A. Kusenko, M. Sasaki and V. Takhistov, *Analytic Description of Primordial Black Hole Formation from Scalar Field Fragmentation*, *JCAP* **10** (2019) 077 [1907.10613].
- [92] M.M. Flores and A. Kusenko, *Primordial black holes as a dark matter candidate in theories with supersymmetry and inflation*, *JCAP* **05** (2023) 013 [2108.08416].
- [93] S. Hawking, *Gravitationally collapsed objects of very low mass*, *Mon. Not. Roy. Astron. Soc.* **152** (1971) 75.